

Title

Evaluation of TOCSY mixing for sensitivity-enhancement in solid-state NMR and application of 4D experiments for side-chain assignments of the full-length 30 kDa membrane protein GlpG

Author information

Carl Öster^{†*}

ORCID: 0000-0002-8723-4533

email: oester@fmp-berlin.de

Veniamin Chevelkov[‡]

ORCID: 0000-0002-7615-3535

Adam Lange^{‡§*}

ORCID: 0000-0002-7534-5973

email: alange@fmp-berlin.de

[†]Research Unit Molecular Biophysics, Leibniz-Forschungsinstitut für Molekulare Pharmakologie, Robert-Rössle-Straße 10, 13125 Berlin, Germany

[§]Institut für Biologie, Humboldt-Universität zu Berlin, Invalidenstraße 42, 10115 Berlin, Germany

*Corresponding authors

Abstract

Chemical shift assignments of large membrane proteins by solid-state NMR experiments are challenging. Recent advancements in sensitivity-enhanced pulse sequences, have made it feasible to acquire ¹H-detected 4D spectra of these challenging protein samples within reasonable timeframes. However, obtaining unambiguous assignments remains difficult without access to side-chain chemical shifts. Drawing inspiration from sensitivity-enhanced TOCSY experiments in solution NMR, we have explored the potential of ¹³C-¹³C TOCSY mixing as a viable option for triple sensitivity-enhanced 4D experiments aimed at side-chain assignments in solid-state NMR. Through simulations and experimental trials, we have identified optimal conditions to achieve uniform transfer efficiency for both transverse components and to minimize undesired cross-transfers. Our experiments, conducted on the 30 kDa membrane protein GlpG embedded in *E. coli* liposomes, have demonstrated enhanced sensitivity compared to the most effective dipolar and J-coupling-based ¹³C-¹³C mixing sequences. Notably, a non-uniformly sampled 4D hCXANH spectrum with exceptionally high sensitivity was obtained in just a few days using a 600 MHz spectrometer equipped with a 1.3 mm probe operating at a magic angle spinning rate of 55 kHz.

Introduction

The recent development of sensitivity-enhanced transverse mixing sequences suitable for ^1H detected solid-state NMR experiments enables fast acquisition of multidimensional experiments for protein backbone assignments. These new sequences include two different approaches, Transverse mixing optimal control pulses (TROP)^{1,2} and simplified preservation of equivalent pathways spectroscopy (SPEPS)^{3,4}. Both allow for simultaneous magnetization transfers of two components, similar to the strategies previously developed for solution NMR experiments^{5,6}, which leads to a theoretical increase in the signal-to-noise ratio (SNR) by a factor of $\sqrt{2}$ per indirect dimension. It is now straight-forward to assemble all sensitivity-enhanced 3D and 4D pulse sequences required to record spectra for assignments of H, N, C α and CO chemical shifts. However, in order to unambiguously assign challenging proteins, access to side chain chemical shifts is critical. Total correlation spectroscopy (TOCSY) mixing was shown to be highly efficient for ^{13}C - ^{13}C transfers at magic angle spinning (MAS) rates of ≥ 100 kHz MAS⁷ and has since then often been applied for side chain assignments of various types of biomolecules⁸⁻¹⁰. The suitability of different homonuclear mixing sequences for side chain assignments in ^1H detected experiments at MAS rates of 55-100 kHz has recently been thoroughly explored¹¹, with the best performing sequences being dipolar recoupling enhancement through amplitude modulation (DREAM)¹², TOCSY (DIPSI-3)¹³ and Total through-bond correlation spectroscopy (TOBSY)^{14,15} (C9₄₈)¹⁶. It is therefore useful to revisit TOCSY mixing sequences that have been shown to enable sensitivity-enhancement in solution NMR experiments⁵. Here we explore the suitability of DIPSI-3 for sensitivity-enhanced solid-state NMR experiments. We first evaluate the approach by performing ^{13}C detected solid-state NMR experiments on a $^{13}\text{C}^{15}\text{N}$ labelled methionine-leucine-phenylalanine (MLF) powder sample in combination with simulations of polarization transfer dynamics. Next, we show that by using DIPSI-3 for ^{13}C - ^{13}C mixing in triple sensitivity-enhanced 4D hCXANH and hXCACoNH experiments (CX represents aliphatic carbon side-chains) we can obtain high quality spectra suitable for side chain assignments in a challenging 30 kDa membrane protein sample, full-length GlpG, in a few days. GlpG is a rhomboid protease that cleaves its substrates within the cell membrane. We have previously investigated the structure and dynamics related to the gating mechanism and inhibitor binding in a truncated version of GlpG (GlpG $_{\Delta\text{N}}$)¹⁷⁻²⁰, where the cytosolic domain has been removed. Additionally, crystal structures of GlpG $_{\Delta\text{N}}$ ^{21,22} and solution NMR structures of the isolated cytosolic domain^{23,24} have been solved. The full length protein has, however, not been characterized in detail so far. As a first step towards the full structural and dynamic characterization of GlpG, we focus here on obtaining the chemical shift assignments of a 100% H₂O back-exchanged $^2\text{H}^{13}\text{C}^{15}\text{N}$ –uniformly labelled protein sample in a lipid bilayer. We combine the sensitivity-enhanced TOCSY spectra with double sensitivity-enhanced 3D hCANH and hCONH and triple sensitivity-enhanced 4D hCACoNH and hCOCANH spectra. The advantages of using high dimensional ($\geq 4\text{D}$) spectra for assignments of challenging proteins by solid-state NMR have been thoroughly explored in several studies^{10,25-28}. Since we are performing the experiments on a perdeuterated sample, we mostly expect to achieve C β assignments from the TOCSY experiments. However, for most residue types all aliphatic carbon side-chains are available for assignments based on triple sensitivity-enhanced 4D hCXANH and hXCACoNH spectra despite that the initial magnetization pool is limited to back-exchanged protons.

Methods

Protein expression and purification

GlpG was expressed, purified and reconstituted into liposomes (*E. coli* total lipid extract (Avanti Lipids)) as previously described¹⁷. The protein to lipid ratio was 1:1 (w/w), corresponding to

approximately 1:44 (mol/mol) and the final buffer condition for the NMR sample was 50 mM Tris-HCl, 150 mM NaCl, 1mM MgCl, pH 7.4.

Solid-state NMR

The protein sample was packed into a 1.3 mm rotor using centrifugation at 10,000 relative centrifugal force in a benchtop centrifuge. 0.2 μ l of a saturated solution of DSS in sample buffer was added to the protein sample before closing the rotor to allow for internal referencing. A thin layer of glue was added to seal the caps (see e.g ref²⁹ for a detailed description of the rotor packing procedure). All solid state NMR experiments were recorded on a 600 MHz spectrometer (Bruker) equipped with a triple channel (HCN) 1.3 mm probe (Bruker) operating at a MAS rate of 55 kHz. ¹³C detected 2D hNCACX spectra were recorded on MLF using a double sensitivity-enhanced hNCACX pulse sequence modified from a previously published hNCACO pulse sequence². Cross-polarization (CP) was used for ¹H-¹⁵N transfers, SPEPS³ for ¹⁵N-¹³C α transfers and TOCSY (DIPSI-3)¹³, TOBSY (C9₄₈)¹⁶ or hSPEPS⁴ for ¹³C α -¹³CX transfers. Experiments on GlpG were performed at a sample temperature of ca 20 °C, based on the chemical shift of the water peak referenced internally to DSS. Standard and sensitivity-enhanced ¹³C detected 2D hCC spectra were recorded using the different mixing sequences mentioned above. 3D and 4D experiments were recorded using sensitivity-enhanced pulse sequences and ¹H detection. CP was used for the first magnetization transfer step (¹H-¹³C α , ¹H-¹³CO or ¹H-¹³CX). TROP shapes specific for 55 kHz MAS were used for ¹³C α -¹⁵N, ¹³CO-¹⁵N, ¹³C α -¹³CO (specific for 600 MHz spectrometer), ¹³CO-¹³C α (specific for 600 MHz spectrometer) and ¹⁵N-¹H transfers. DIPSI-3 was used for ¹³CX-¹³C α transfers. 3D hCANH and hCONH spectra were recorded in a uniform fashion and processed using TopSpin v4 (Bruker). 4D spectra were recorded using 5 % non-uniform sampling (NUS). Two additional 3D hCXcaNH spectra, one with TOCSY mixing and one with hSPEPS mixing, were recorded using 25% NUS. 10 kHz Waltz-64³⁰ decoupling was applied to the ¹H channel during acquisition of the indirect dimensions and on the ¹⁵N and ¹³C channels during direct ¹H acquisition. MISSISSIPPI³¹ was used for water suppression. Echo-Antiecho was used for all indirect dimensions in sensitivity-enhanced experiments and States-TPPI³² was used in standard experiments. All sensitivity-enhanced pulse sequences were modified based on previously published sensitivity-enhanced pulse sequences to allow for additional dimensions to be recorded and to introduce ¹³C-¹³C mixing for side-chain assignments. A scheme of the sensitivity-enhanced hCXCANH pulse sequence is provided in SI Fig. 1. Original pulse sequences and TROP shapes were downloaded from www.optimal-nmr.net^{1,2}. NUS lists were generated from <http://gwagner.med.harvard.edu/intranet/hmslST>^{33,34}. NUS spectra were reconstructed and processed using nmrPipe³⁵. Experimental details for all assignment spectra are provided in SI tables 1-2. Processing details for NUS spectra are provided in SI table 3 and details for the conversion from Bruker to nmrPipe format is shown in SI figure 2. CCPNMR AnalysisAssign v3.1³⁶ was used for data analysis, assignments and to generate figures of multidimensional NMR spectra.

Simulations

The software package SIMPSON 4.2.1³⁷ was used to simulate polarization transfer dynamics between different components of two ¹³C spins representing C α and C β nuclei for DIPSI-3, hSPEPS^{CA-CB} and C9₄₈¹ recoupling sequences. Homonuclear dipolar and scalar couplings were set to 2084.9 Hz and 35 Hz respectively. Isotropic chemical shifts for C α and C β nuclei were 52 ppm and 22 ppm, while radio-frequency (RF) irradiation was applied at 37 ppm. Numerical studies were performed for 55 kHz MAS rate and 600 MHz spectrometer. The RF field strength for DIPSI-3 was set to 10 kHz, while it was set according to the MAS rate for hSPEPS^{CA-CB} (27.5 kHz average RF strength) and C9₄₈¹ (20.625 kHz RF strength). Selected sections of the SIMPSON input file, which represent relevant computational and interaction parameters are given in the supplementary information (supplementary text). The

simulations explore polarization transfer efficiency between principal components of $C\alpha$ and $C\beta$ spins, (i.e. X to X, Y to Y, Z to Z). Additionally, undesirable mixing between orthogonal magnetization components (i.e. X and Y, X and Z etc.), which, in principle, could give rise to phase distortions and/or artefacts in the spectra was systematically explored. Finally, we analysed the effects of RF inhomogeneity on the performance of the considered pulse sequences.

Results and discussion

Evaluation of the suitability of DIPSI-3 for sensitivity-enhanced solid-state NMR experiments

To evaluate the suitability of DIPSI-3 for use in sensitivity-enhanced solid-state NMR experiments, we recorded 2D hnCACX spectra of $^{13}\text{C}^{15}\text{N}$ labelled MLF at 55 kHz MAS. We tested two different approaches for DIPSI-3, with and without 90 degree pulses before and after the DIPSI-3 mixing. The difference between these approaches is that if we include 90 degree pulses with the phase x and -x, while the DIPSI-3 spin-lock is along y (from now on referred to as zTOCSY), the two components that are preserved are Z and X and if we don't include the 90 degree pulses (from now on referred to as xyTOCSY) the preserved components are X and Y. Using zTOCSY (orange spectrum in Fig. 1B) with 16.3 ms mixing time at a nutation frequency of 10 kHz results in a spectrum where cross-peaks with the $C\alpha$ carbons appear for all expected side-chain carbons. With the xyTOCSY approach all expected peaks also appear (brown spectrum in Fig. 1B), but some mirrored peaks with opposite phase compared to the real peaks can also be observed (grey peaks with red crosses). To further explore the appearance of mirrored peaks we recorded the same spectrum using TOBSY (C9_{48})¹⁶ (green spectrum in Fig. 1B, from now on referred to as C9) that allows for non-negligible cross-transfer (e.g. X-Y, X-Z etc.). C9 shows efficient transfer to all expected side-chains (indicated with black crosses) and additionally strong mirrored peaks (indicated with red crosses) when the spectrum is recorded in a sensitivity-enhanced fashion. In standard experiments unwanted cross-transfers can be compensated for by using a z-filter, which is typically done for applications of C9 sequences^{16,38}. However, applying a z-filter is not compatible with sensitivity-enhanced experiments since then only one component would be preserved. During the preparation of this manuscript a new approach using dipolar-based ^{13}C - ^{13}C mixing (homonuclear SPEPS) was published⁴. In addition to backbone homonuclear transfers ($^{13}\text{C}\alpha$ - $^{13}\text{C}\text{O}$, $^{13}\text{C}\text{O}$ - $^{13}\text{C}\alpha$), a mixing sequence for $^{13}\text{C}\alpha$ - $^{13}\text{C}\beta$ transfers (homonuclear SPEPS^{CA-CB}, from now on referred to as hSPEPS) suitable for sensitivity-enhanced experiments was reported. We include this mixing sequence as a dipolar based alternative, instead of DREAM¹² that is not compatible with sensitivity-enhancement. As expected, hSPEPS mixing leads to a spectrum with strong $C\beta$ - $C\alpha$ cross-peaks without any mirrored peaks. A comparison of the transfer efficiency for the different mixing sequences (Fig. 1 C) reveals that hSPEPS performs best for $C\alpha$ - $C\beta$ transfers, while C9 performs best for other side-chains (slightly better than zTOCSY followed by xyTOCSY). The phenylalanine of MLF was not included in the comparison since the ^{13}C offset for the indirect dimension is at the $C\alpha$ chemical shift of the phenylalanine leading to that mirrored peaks will overlap with real peaks and a reliable characterization of the peak intensities is not possible. Note that hSPEPS also allows for transfer to carbons further down the side-chain if a longer mixing time is used⁴, but with lower efficiency compared to TOCSY and C9 (see SI figure 3). The main reason for unwanted cross-transfers resulting in mirrored peaks appears to be inhomogeneity of RF pulses or rather the robustness of the mixing sequences towards RF inhomogeneity. This was realized based on SIMPSON³⁷ simulations of the transfer efficiencies for transfers between all possible components at different mixing times. RF inhomogeneity was tested by varying the RF power in the simulations by 10% from the ideal conditions. Fig. 1D shows a bar plot summarizing the results from the simulations of DIPSI-3 and Fig. 1E shows examples of the results from the full simulations. The transfer efficiency pattern for the X and Z components are very similar ($C\alpha_z$ to $C\beta_z$ and $C\alpha_x$ to $C\beta_x$). The unwanted $C\alpha_x$ to $C\beta_z$ and $C\alpha_z$ to $C\beta_x$ cross-transfers are minimal while the $C\alpha_x$ to $C\beta_y$ and $C\alpha_y$ to $C\beta_x$ cross-transfers

are non-negligible. This becomes clear when non-ideal RF powers are applied (red and yellow bars and lines in Fig. 1D). The simulations agree well with the experimental data regarding unwanted cross-transfers resulting in mirrored peaks, see supplementary information for the results from all simulations of DIPSI-3 (SI Fig. 4), C9₄₈¹ (SI Fig. 5) and hSPEPS (SI Fig. 6). A comparison of the intensities of the peaks in the zTOCSY and xyTOCSY spectra (Fig. 1C) shows that the sensitivities of the C α -CX peaks are not strongly affected by unwanted cross-transfers in MLF, although any loss of sensitivity and the appearance of mirrored peaks would be problematic for protein chemical shift assignments.

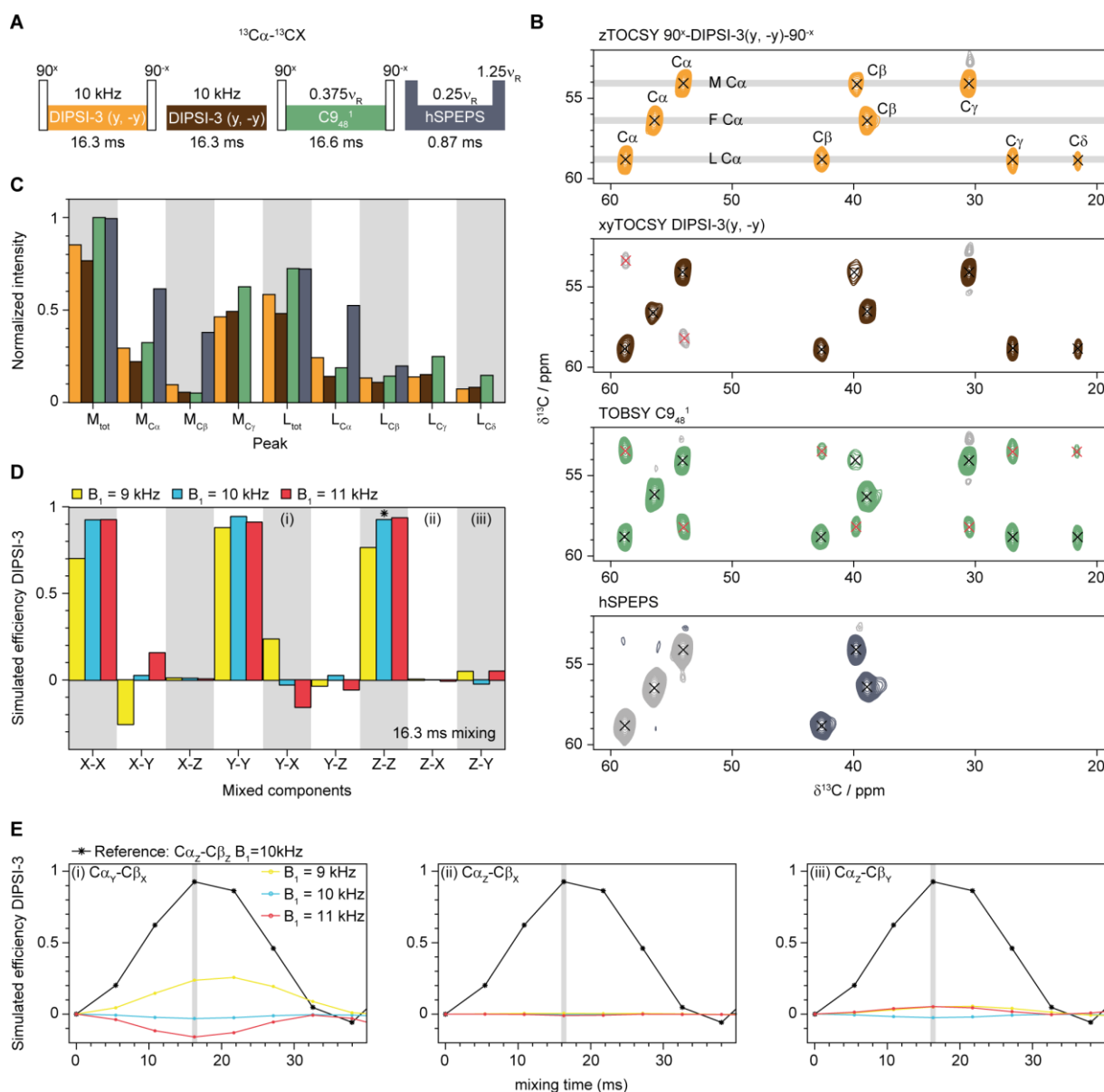


Figure 1. Evaluation of the suitability for sensitivity-enhancement of the DIPSI-3 mixing sequence on MLF. (A) Scheme of ^{13}C - ^{13}C mixing sequences (DIPSI-3, C9₄₈¹, and hSPEPS). (B) Sensitivity-enhanced 2D hnCACX spectra of $^{13}\text{C}^{15}\text{N}$ labelled MLF recorded at 55 kHz MAS on a 600 MHz spectrometer using the different ^{13}C - ^{13}C mixing sequences. Black crosses represent wanted peaks (assignments shown in the spectrum at the top) and red crosses represent mirrored peaks originating from unwanted cross-transfers. (C) Comparison of peak intensities in the spectra resulting from the different mixing sequences. The peak intensities are normalized to the highest intensity (the combined intensity for all peaks of the methionine (M_{tot}) in the C9 spectrum). The colour coding is the same in panels A, B and C. (D) Bar plot summarizing the simulated transfer efficiencies of DIPSI-3 under the same conditions as in the experiments (16.3 ms mixing). Radio-frequency inhomogeneity is simulated by varying the nutation frequency by $\pm 10\%$ from the ideal conditions (10 kHz). (E) Example plots representing the full simulations of DIPSI-3 for C α_x to C β_x (left, (i)), C α_z to C β_x (middle, (ii)) and C α_z to C β_y (right, (iii)). The grey shaded bars in E represent the values at 16.3 ms mixing, these are indicated in the bar plot in panel D ((i), (ii) and (iii)). The colour coding is the same in panels D and E.

Evaluation of ^{13}C - ^{13}C mixing sequences on GlpG

Based on the experiments on MLF and the simulations of the mixing sequences, the best approach for sensitivity-enhanced solid-state NMR experiments for C β assignments appears to be hSPEPS and for side-chain assignments further than C β the zTOCSY approach (at 55 kHz MAS and on a 600 MHz spectrometer). Next we evaluated the transfer efficiency on a 100% H $_2$ O back-exchanged $^2\text{H}^{13}\text{C}^{15}\text{N}$ labelled GlpG sample at 55 kHz MAS. Figure 2A shows extracted regions of ^{13}C detected 2D hCC spectra using sensitivity-enhanced (using Echo-Antiecho) and standard (using States-TPPI) pulse sequences. A comparison of the peak intensities between sensitivity-enhanced and standard zTOCSY experiments (orange vs purple in Fig. 2B) shows the expected increase in peak intensities by approximately a factor of 2 in the sensitivity-enhanced experiment, which corresponds to an increase in SNR by $\sqrt{2}$. We also compared the peak intensities to a spectrum recorded with standard acquisition using C9 for ^{13}C - ^{13}C mixing (green in Fig. 2) and a spectrum recorded using sensitivity-enhanced hSPEPS (dark grey in Fig. 2). For most peaks investigated in GlpG, the sensitivity-enhanced zTOCSY shows the highest intensity (Fig. 2B) and, as expected, it also gives additional peaks coming from carbons further down the side-chain compared to hSPEPS (Fig. 2A, see also SI Fig. 7 for the full spectra).

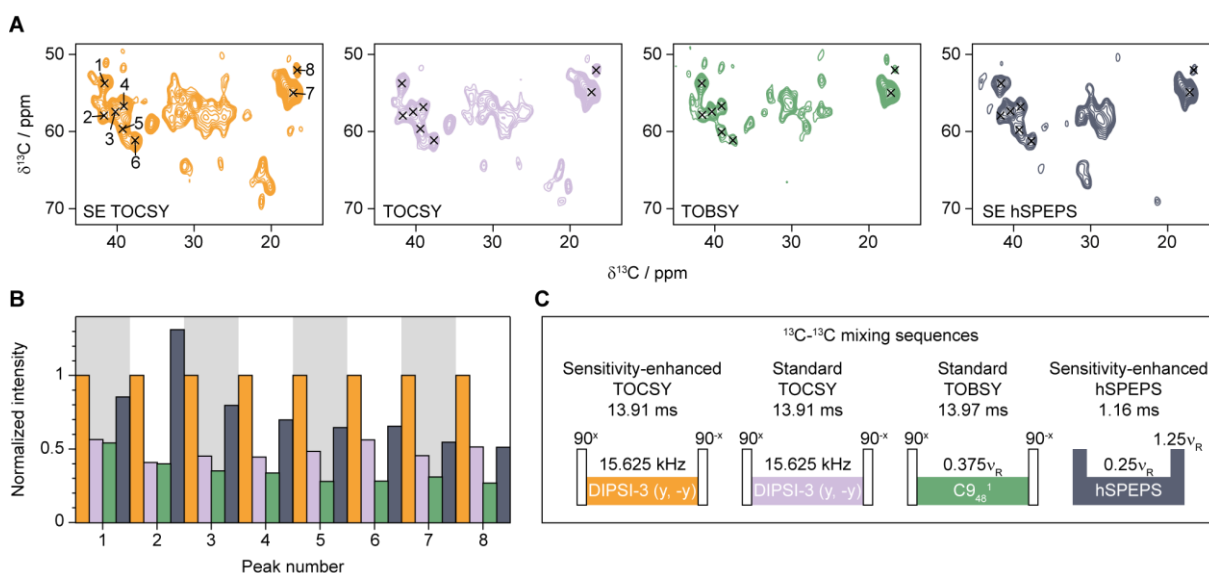


Figure 2. Evaluation of DIPSI-3 mixing on $^2\text{H}^{13}\text{C}^{15}\text{N}$ labelled GlpG. (A) 2D hCC spectra recorded at 55 kHz MAS on a 600 MHz spectrometer using sensitivity-enhanced and standard experiments with different ^{13}C - ^{13}C mixing sequences. Black crosses represent peaks used for comparison. (B) Normalized peak intensities for 8 different peaks that can be identified in all spectra. (C) Schematic drawing of the ^{13}C - ^{13}C mixing sequences used. The same colour coding is used in all panels.

Chemical shift assignment of full length GlpG

Despite access to chemical shift assignments of the isolated transmembrane (solid-state NMR¹⁷) and cytosolic (solution NMR^{23,24}) domains, the assignment of full length GlpG (276 residues) is not trivial. Several peaks are overlapping in 3D spectra and there are many regions where the chemical shifts differ significantly between the full length protein and the isolated domains. The possibility to acquire triple sensitivity-enhanced 4D experiments, enabled by the recent development of TROP and SPEPS pulses, simplified the assignment procedure considerably. Here we used TROP for backbone ^{13}C - ^{15}N , ^{13}C - ^{13}C and ^{15}N - ^1H transfers (see SI Fig. 8 for example strip plots of the backbone spectra). It should be mentioned that the TROP ^{15}N - ^1H transfer is less efficient compared to CP for GlpG (see SI

Fig. 9 for a comparison of 1D spectra), but due to the combined sensitivity-enhancement from each indirect dimension it is still possible to record highly sensitive 4D spectra in a reasonable time. Triple sensitivity-enhanced 4D hCACONH and hCOCANH were recorded in ca 48 hours each, hCXCANH in ca 100 hours and hCXCAcoNH in ca 170 hours. All 4D spectra were recorded at 55 kHz MAS on a 600 MHz spectrometer, using 5% NUS. The experiments for chemical shift assignments were performed on a back-exchanged perdeuterated sample. This makes experiments for side-chain assignments challenging since the pool of initial magnetization in the ^1H - ^{13}C CP step is limited to back-exchanged sites, mostly amide protons. With this in mind the main goal was to obtain $\text{C}\beta$ assignments. Unambiguous assignments of GlpG would not be possible without access to at least $\text{C}\beta$ chemical shifts, additional side-chain information is of course highly beneficial. The initial ^1H - ^{13}C CP was optimized for highest intensity in the region around 10-40 ppm, where most $\text{C}\beta$ and other expected side-chains appear. Longer mixing time could potentially improve the side-chain assignments of carbon atoms further down the side-chain, but will lead to an overall loss in sensitivity. Figure 3B shows an example of side-chain assignments for residues W38-Q44 based on the sensitivity-enhanced 4D TOCSY experiments, Fig. 3A shows how the spectra are connected in the strip plots. All the $\text{C}\beta$ chemical shifts of residues W38-Q44 could be assigned and, additionally, the $\text{C}\gamma$ chemical shifts of E42 and Q44 were also assigned. But for the leucine residue (L39), with a hydrophobic branched side-chain, only the $\text{C}\beta$ was visible in the spectra. Figure 3C shows an AlphaFold2^{39,40} model of GlpG with the residues coloured depending on the assignments (see SI tables 4 to 6 for assigned chemical shifts). In total, utilizing sensitivity-enhanced 3D and 4D spectra for backbone and side-chain assignments, the $\text{C}\alpha$ chemical shifts of 133 residues were successfully assigned (137 residues with any atom assigned). Among these, fifteen residues are glycines and prolines, leaving 118 residues for potential side-chain assignments. Of these, the $\text{C}\beta$ chemical shifts were assigned in 91 residues (green in Fig. 3C), while in 7 residues where the $\text{C}\beta$ could not be assigned, another side-chain was assigned (orange in Fig. 3C). Consequently, only 20 residues remain without any side-chain assignments (dark gray in Fig. 3C). Figure 3D provides a comprehensive analysis of side-chain assignments for each residue type in GlpG, excluding glycine and proline. Side-chains that were consistently assigned are denoted in green, those occasionally assigned in orange, and those not assigned in red. This pattern aligns relatively well with expected outcomes for side-chain assignments in a perdeuterated sample, where $\text{C}\beta$ chemical shifts are typically available to be assigned, and carbons further along the side-chain are less frequently assignable. Notable exceptions where $\text{C}\beta$ was not consistently assigned include glutamates (3/8), threonines (2/6), and valines (1/10). For glutamates, the missing assignments appear to be due to the residues' positioning within the protein. For example, two of the glutamates lacking $\text{C}\beta$ assignments (E118 and E166) are residues where the amide protons could not be assigned, but the $\text{C}\alpha$ (and CO) chemical shifts were determined using the amide protons of the preceding residues in the 4D hCACONH spectrum. The reason for the lack of $\text{C}\beta$ assignments of several threonines remains unclear, especially since the $\text{C}\gamma$ were assigned in 5 out of 6 threonines. The sole threonine with a missing $\text{C}\gamma$ assignment is T97, which is similarly situated as E118 and E166. A plausible explanation for the missing threonine $\text{C}\beta$ assignments could be unfavorable dynamics, resulting in inadequate coherence lifetimes for the many magnetization transfer steps in the 4D TOCSY experiments, while the fast-moving methyl groups ($\text{C}\gamma$) have longer coherence lifetimes, thus detectable in TOCSY experiments. Another possible reason is the close similarity between $\text{C}\alpha$ and $\text{C}\beta$ chemical shifts in some threonines, hindering their distinction. Valines, expected to behave similarly to other residues with branched hydrophobic side-chains such as leucines and isoleucines, showed an unexpected pattern, with only 1 out of 10 valine $\text{C}\beta$ assigned. There is no apparent explanation for this discrepancy. Future structural and dynamic studies of GlpG may elucidate why the valine side-chains are challenging to assign. Intriguingly, among the side-chains within the TOCSY mixing range, the only ones never appearing in the spectra are the $\text{C}\gamma$ and $\text{C}\delta$

of isoleucines and leucines, and the $C\epsilon$ of lysines (see Fig. 3D). This implies that nearly complete side-chain assignments are achievable using sensitivity-enhanced TOCSY experiments in solid-state NMR of perdeuterated proteins at 55 kHz. Given the complexity of GlpG as a membrane protein, numerous factors could contribute to the difficulty in assigning certain residues, such as unfavourable dynamics, lipid interactions, incomplete back-exchange of exchangeable protons, and overlapping peaks.

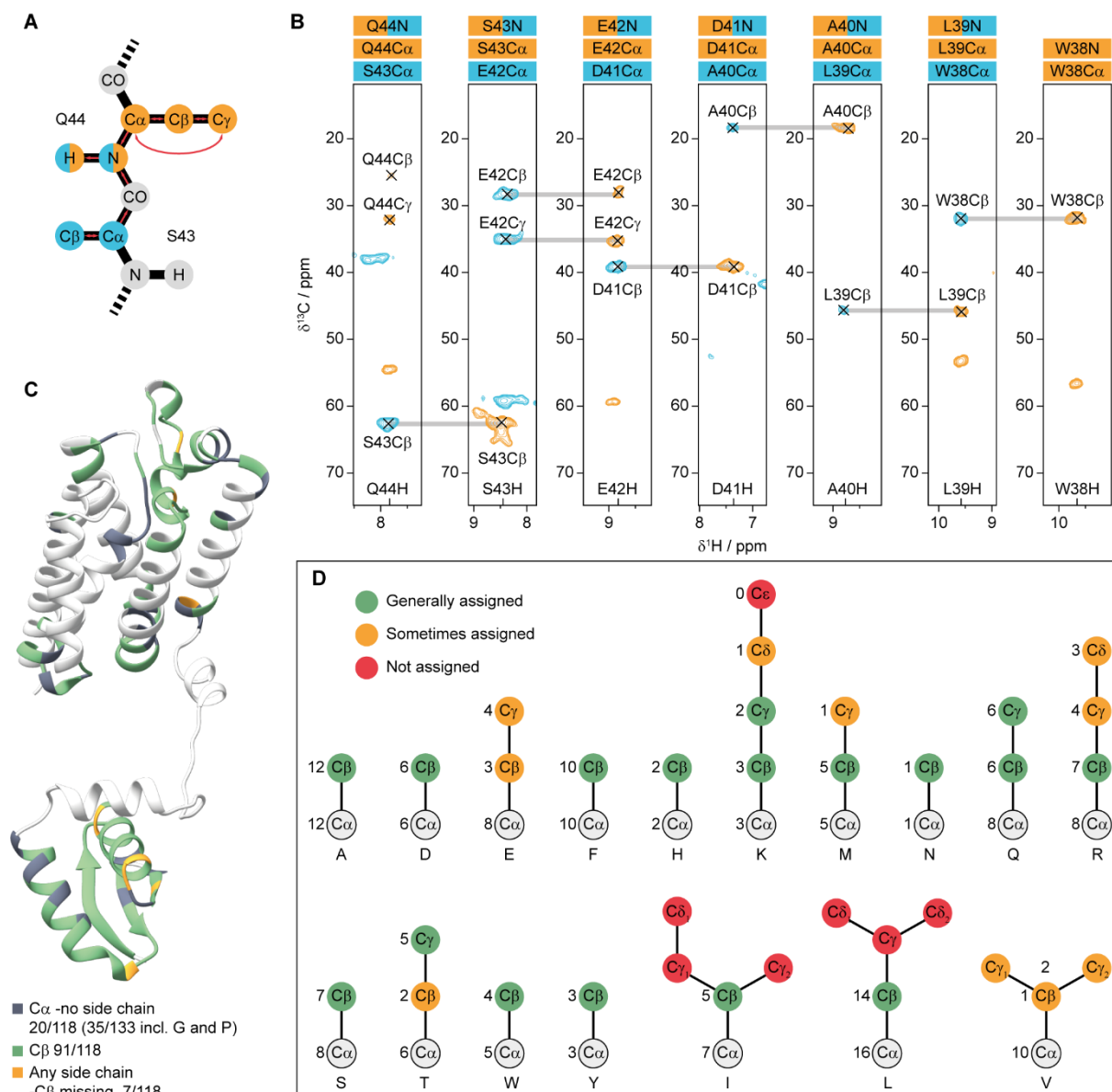


Figure 3. Summary of the side chain assignments enabled by the triple sensitivity-enhanced 4D experiments. (A) Scheme of how the resonances are visualized in the strip plots with the magnetization transfer pathways indicated (red arrows). (B) Strip plots for the region Q44 to W38, showing the side-chain assignments for residue *i* in orange (hCxCaNH) and *i*-1 in blue (hCxCaOxNH) connected to the backbone ^{15}N and ^1H resonances of residue *i*. (C) Summary of the side-chain assignments plotted onto a model of GlpG. Residues with C α but no side chain assignments are coloured in dark gray, residues with C β assignments are coloured in green and residues with no C β assignments but with other carbon side-chains assigned are coloured in orange. (D) Scheme summarizing the side chain assignments for each residue type found in GlpG (except glycines and prolines). Green circles indicate side-chains that were generally assigned, orange circles represent side-chains that were sometimes assigned and red circles represent side-chains that could not be assigned.

Leveraging the high performance of the newly developed hSPEPS for dipolar-based $^{13}\text{C}\beta$ - $^{13}\text{C}\alpha$ transfers, we assessed whether the extended mixing time and reliance on J-coupling transfers in TOCSY could explain some missing C β assignments. We recorded double sensitivity-enhanced 3D

hCXcaNH spectra employing hSPEPS and zTOCSY. However, no additional C β peaks, unassigned in the 4D TOCSY spectra, were identified in the 3D hSPEPS spectrum. A comparative analysis of the intensities of isolated C β -N-H peaks in the 3D spectra indicated that zTOCSY generally outperformed hSPEPS (see SI Fig. 9). This suggests that the TOCSY-based approach is suitable for membrane proteins, and the missing side-chain assignments in GlpG are likely attributed to internal dynamics and lipid-protein interactions interfering with both dipolar and J-coupling-based magnetization transfers.

Concluding remarks

This study demonstrates the efficiency of ^{13}C - ^{13}C TOCSY mixing via the DIPSI-3 mixing sequence for sensitivity-enhanced solid-state NMR experiments. 90 degree pulses before and after the DIPSI-3 mixing sequence are important to prevent unwanted cross-transfers resulting in mirrored peaks and loss of sensitivity. The methodology can be seamlessly integrated with advanced sensitivity-enhanced mixing sequences, such as TROP and SPEPS, which facilitate transfers between backbone atoms. Consequently, it enables the construction of sensitivity-enhanced 4D experiments, thereby facilitating the side-chain assignments of complex membrane proteins. We validated this approach using a back-exchanged perdeuterated protein sample of the full length 30 kDa membrane protein GlpG. A comprehensive dataset, suitable for backbone and side-chain assignments, comprising two double sensitivity-enhanced 3D spectra and four triple sensitivity-enhanced 4D spectra was acquired within a three-week period at 55 kHz MAS on a 600 MHz spectrometer. Interestingly, despite utilizing a back-exchanged perdeuterated sample, all anticipated side-chain carbons for all residue types, excluding the C γ and C δ of isoleucines and leucines and the C ϵ of lysines, were detectable. This approach should prove even more advantageous for proteins with higher degrees of side-chain protonation that enables more efficient ^1H - ^{13}C magnetization transfers compared to back-exchanged perdeuterated samples, provided that sufficiently fast MAS rates and/or high external magnetic field strengths are applied.

Author contributions

Conceptualization: C.Ö. Methodology: C.Ö., V.C. Software: C.Ö., V.C. Validation: C.Ö., V.C. Formal analysis: C.Ö., V.C. Investigation: C.Ö., V.C. Resources: A.L. Data curation: C.Ö., V.C. Writing - Original Draft: C.Ö. Writing - Review & Editing: C.Ö., V.C., A.L. Visualization: C.Ö., V.C. Supervision: A.L. Project Administration: C.Ö., A.L. Funding acquisition: A.L.

Acknowledgements

We thank Susanne Bischoff and Sascha Lange for assistance with the production of an isotope labelled protein sample, Jan Blahut for helpful discussions about TROP and Loren Andreas and Evgeny Nimerovsky for helpful discussions about SPEPS.

Declarations

Funding

This work was supported by the Leibniz-Forschungsinstitut für Molekulare Pharmakologie (FMP) and the Deutsche Forschungsgemeinschaft (DFG, German Research Foundation) under Germany's Excellence Strategy – EXC 2008/1 (UniSysCat) – 390540038 (to A.L.).

Competing Interest

The authors have no conflicts of interest to declare that are relevant to the content of this article.

Data availability

The chemical shift assignments of GlpG are available in the supplementary information and deposited to the BMRB under accession number 52584. All information needed to reproduce the experiments in this study is included in the article and supplementary information. Further inquiries are available from the corresponding authors upon reasonable request.

References

1. Blahut, J., Brandl, M. J., Pradhan, T., Reif, B. & Tošner, Z. Sensitivity-Enhanced Multidimensional Solid-State NMR Spectroscopy by Optimal-Control-Based Transverse Mixing Sequences. *J. Am. Chem. Soc.* **144**, 17336–17340 (2022).
2. Blahut, J., Brandl, M. J., Sarkar, R., Reif, B. & Tošner, Z. Optimal control derived sensitivity-enhanced CA-CO mixing sequences for MAS solid-state NMR – Applications in sequential protein backbone assignments. *J. Magn. Reson. Open* **16–17**, 100122 (2023).
3. Nimerovsky, E., Varkey, A. C., Kim, M., Becker, S. & Andreas, L. B. Simplified Preservation of Equivalent Pathways Spectroscopy. *JACS Au* **3**, 2763–2771 (2023).
4. Nimerovsky, E. *et al.* Homonuclear Simplified Preservation of Equivalent Pathways Spectroscopy. *J. Phys. Chem. Lett.* **15**, 6272–6278 (2024).
5. Cavanagh, J. & Rance, M. Sensitivity improvement in isotropic mixing (TOCSY) experiments. *J. Magn. Reson.* **88**, 72–85 (1990).
6. Schleucher, J., Sattler, M. & Griesinger, C. Coherence Selection by Gradients without Signal Attenuation: Application to the Three-Dimensional HNC0 Experiment. *Angew. Chemie Int. Ed. English* **32**, 1489–1491 (1993).
7. Stanek, J. *et al.* NMR Spectroscopic Assignment of Backbone and Side-Chain Protons in Fully Protonated Proteins: Microcrystals, Sedimented Assemblies, and Amyloid Fibrils. *Angew. Chemie Int. Ed.* **55**, 15504–15509 (2016).
8. Öster, C. *et al.* Structural studies suggest aggregation as one of the modes of action for teixobactin. *Chem. Sci.* **9**, 8850–8859 (2018).
9. Marchanka, A., Stanek, J., Pintacuda, G. & Carlomagno, T. Rapid access to RNA resonances by proton-detected solid-state NMR at >100 kHz MAS. *Chem. Commun.* **54**, 8972–8975 (2018).
10. Klein, A., Vasa, S. K., Söldner, B., Grohe, K. & Linser, R. Unambiguous Side-Chain Assignments for Solid-State NMR Structure Elucidation of Nondeuterated Proteins via a Combined 5D/4D Side-Chain-to-Backbone Experiment. *J. Phys. Chem. Lett.* **13**, 1644–1651 (2022).
11. Paluch, P. *et al.* NMR Assignment of Methyl Groups in Immobilized Proteins Using Multiple-Bond ¹³C Homonuclear Transfers, Proton Detection, and Very Fast MAS. *Front. Mol. Biosci.* **9**, 1–18 (2022).
12. Verel, R., Ernst, M. & Meier, B. H. Adiabatic Dipolar Recoupling in Solid-State NMR: The DREAM Scheme. *J. Magn. Reson.* **150**, 81–99 (2001).
13. Shaka, A. ., Lee, C. . & Pines, A. Iterative schemes for bilinear operators; application to spin decoupling. *J. Magn. Reson.* **77**, 274–293 (1988).
14. Baldus, M. & Meier, B. H. Total Correlation Spectroscopy in the Solid State. The Use of Scalar Couplings to Determine the Through-Bond Connectivity. *J. Magn. Reson. Ser. A* **121**, 65–69 (1996).
15. Baldus, M., Iulicucci, R. J. & Meier, B. H. Probing Through-Bond Connectivities and Through-

- Space Distances in Solids by Magic-Angle-Spinning Nuclear Magnetic Resonance. *J. Am. Chem. Soc.* **119**, 1121–1124 (1997).
16. Tan, K. O. *et al.* Efficient low-power TOBSY sequences for fast MAS. *Solid State Nucl. Magn. Reson.* **89**, 27–34 (2018).
 17. Shi, C. *et al.* Structure and Dynamics of the Rhomboid Protease GlpG in Liposomes Studied by Solid-State NMR. *J. Am. Chem. Soc.* **141**, 17314–17321 (2019).
 18. Bohg, C. *et al.* A combination of solid-state NMR and MD simulations reveals the binding mode of a rhomboid protease inhibitor. *Chem. Sci.* **12**, 12754–12762 (2021).
 19. Bohg, C. *et al.* The opening dynamics of the lateral gate regulates the activity of rhomboid proteases. *Sci. Adv.* **9**, 1–11 (2023).
 20. Chevelkov, V., Lange, S., Sawczyk, H. & Lange, A. Accurate Determination of Motional Amplitudes in Biomolecules by Solid-State NMR. *ACS Phys. Chem. Au* **3**, 199–206 (2023).
 21. Wang, Y., Zhang, Y. & Ha, Y. Crystal structure of a rhomboid family intramembrane protease. *Nature* **444**, 179–180 (2006).
 22. Wu, Z. *et al.* Structural analysis of a rhomboid family intramembrane protease reveals a gating mechanism for substrate entry. *Nat. Struct. Mol. Biol.* **13**, 1084–1091 (2006).
 23. Sherratt, A. R., Blais, D. R., Ghasriani, H., Pezacki, J. P. & Goto, N. K. Activity-based protein profiling of the escherichia coli GlpG rhomboid protein delineates the catalytic core. *Biochemistry* **51**, 7794–7803 (2012).
 24. Ghasriani, H. *et al.* Micelle-Catalyzed Domain Swapping in the GlpG Rhomboid Protease Cytoplasmic Domain. *Biochemistry* **53**, 5907–5915 (2014).
 25. Xiang, S., Chevelkov, V., Becker, S. & Lange, A. Towards automatic protein backbone assignment using proton-detected 4D solid-state NMR data. *J. Biomol. NMR* **60**, 85–90 (2014).
 26. Xiang, S., Biernat, J., Mandelkow, E., Becker, S. & Linser, R. Backbone assignment for minimal protein amounts of low structural homogeneity in the absence of deuteration. *Chem. Commun.* **52**, 4002–4005 (2016).
 27. Fraga, H. *et al.* Solid-State NMR H–N–(C)–H and H–N–C–C 3D/4D Correlation Experiments for Resonance Assignment of Large Proteins. *ChemPhysChem* **18**, 2697–2703 (2017).
 28. Zinke, M. *et al.* Bacteriophage Tail-Tube Assembly Studied by Proton-Detected 4D Solid-State NMR. *Angew. Chemie Int. Ed.* **56**, 9497–9501 (2017).
 29. Öster, C., Lange, S., Hendriks, K. & Lange, A. Detecting Bound Ions in Ion Channels by Solid-State NMR Experiments on ¹⁵N-Labelled Ammonium Ions. in *Methods in Molecular Biology* **2796**, 23–34 (2024).
 30. Zhou, Z. *et al.* A new decoupling method for accurate quantification of polyethylene copolymer composition and triad sequence distribution with ¹³C NMR. *J. Magn. Reson.* **187**, 225–233 (2007).
 31. Rienstra, C. M., Zhou, D. H. & Rienstra, C. M. High-performance solvent suppression for proton detected solid-state NMR. *J. Magn. Reson.* **192**, 167–72 (2008).
 32. Marion, D., Ikura, M., Tschudin, R. & Bax, A. Rapid recording of 2D NMR spectra without phase cycling. Application to the study of hydrogen exchange in proteins. *J. Magn. Reson.* **85**, 393–399 (1989).
 33. Hyberts, S. G., Milbradt, A. G., Wagner, A. B., Arthanari, H. & Wagner, G. Application of

- iterative soft thresholding for fast reconstruction of NMR data non-uniformly sampled with multidimensional Poisson Gap scheduling. *J. Biomol. NMR* **52**, 315–327 (2012).
34. Hyberts, S. G., Takeuchi, K. & Wagner, G. Poisson-Gap Sampling and Forward Maximum Entropy Reconstruction for Enhancing the Resolution and Sensitivity of Protein NMR Data. *J. Am. Chem. Soc.* **132**, 2145–2147 (2010).
 35. Delaglio, F. *et al.* NMRPipe: A multidimensional spectral processing system based on UNIX pipes. *J. Biomol. NMR* **6**, (1995).
 36. Skinner, S. P. *et al.* CcpNmr AnalysisAssign: a flexible platform for integrated NMR analysis. *J. Biomol. NMR* **66**, 111–124 (2016).
 37. Bak, M., Rasmussen, J. T. & Nielsen, N. C. SIMPSON: A General Simulation Program for Solid-State NMR Spectroscopy. *J. Magn. Reson.* **147**, 296–330 (2000).
 38. Callon, M. *et al.* High and fast: NMR protein–proton side-chain assignments at 160 kHz and 1.2 GHz. *Chem. Sci.* **14**, 10824–10834 (2023).
 39. Jumper, J. *et al.* Highly accurate protein structure prediction with AlphaFold. *Nature* **596**, 583–589 (2021).
 40. Varadi, M. *et al.* AlphaFold Protein Structure Database in 2024: providing structure coverage for over 214 million protein sequences. *Nucleic Acids Res.* **52**, D368–D375 (2024).